Science of the Total Environment 796 (2021) 148905

Contents lists available at ScienceDirect

Science of the Total Environment

journal homepage: www.elsevier.com/locate/scitotenv

Prevalence of SARS-CoV-2 genes in water reclamation facilities: From influent to anaerobic digester

Bishav Bhattarai [a], Sierra Quinn Sahulka [a], Aditi Podder [a], Soklida Hong [a], Hanyan Li [a], Eddie Gilcrease [a], Alex Beams [b], Rebecca Steed [c], Ramesh Goel [a,*]

[a] Department of Civil and Environmental Engineering, University of Utah, UT, USA
[b] Department of Mathematics, University of Utah, UT, USA
[c] Department of Geography, University of Utah, UT, USA

HIGHLIGHTS

- Primary sludge provided a better prediction of disease burden in the sewershed.
- SARS-CoV-2 gene copy numbers were detected in anaerobically digested sludge.
- Low gene copy number were detected at higher temperature.
- Low gene copy numbers were detected at higher pH values.

GRAPHICAL ABSTRACT

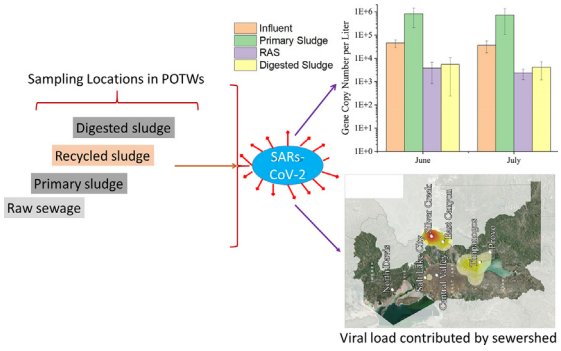

ARTICLE INFO

Article history:
Received 9 April 2021
Received in revised form 21 June 2021
Accepted 4 July 2021
Available online 6 July 2021

Editor: Yifeng Zhang

Keywords:
SARs-CoV-2
Biosolids
Epidemiology
Anaerobic digester
Raw influent
Primary sludge
Disease surveillance

ABSTRACT

Several treatment plants were sampled for influent, primary clarifier sludge, return activated sludge (RAS), and anaerobically digested sludge throughout nine weeks during the summer of the COVID-19 pandemic. Primary clarifier sludge had a significantly higher number of SARS-CoV-2 gene copy number per liter (GC/L) than other sludge samples, within a range from 1.0×10^5 to 1.0×10^6 GC/L. Gene copy numbers in raw influent significantly correlated with gene copy numbers in RAS in Silver Creek (p-value = 0.007, $R^2 = 0.681$) and East Canyon (p-value = 0.009, $R^2 = 0.775$) WRFs; both of which lack primary clarifiers or industrial pretreatment processes. This data indicates that SARS-CoV-2 gene copies tend to partition into primary clarifier sludges, at which point a significant portion of them are removed through sedimentation. Furthermore, it was found that East Canyon WRF gene copy numbers in influent were a significant predictor of daily cases (p-value = 0.0322, $R^2 = 0.561$), and gene copy numbers in RAS were a significant predictor of weekly cases (p-value = 0.0597, $R^2 = 0.449$). However, gene copy numbers found in primary sludge samples from other plants significantly predicted the number of COVID-19 cases for the following week ($t = 2.279$) and the week after that ($t = 2.122$) respectively. These data indicate that SARS-CoV-2 extracted from WRF biosolids may better suit epidemiological monitoring that exhibits a time lag. It also supports the observation that primary sludge removes a significant portion of SARS-CoV-2 marker genes. In its absence, RAS can also be used to predict the number of COVID-19 cases due to direct flow through from influent. This research represents the first of its kind to thoroughly examine SARS-CoV-2 gene copy numbers in biosolids throughout the wastewater treatment process and the relationship between primary, return activated, and anaerobically digested sludge and reported positive COVID-19 cases.

* Corresponding author.
E-mail address: ram.goel@utah.edu (R. Goel).

https://doi.org/10.1016/j.scitotenv.2021.148905
0048-9697/

1. Introduction

As of June 12th, 2021, a severe acute respiratory syndrome (SARS)-the related disease has infected over 176 million people and caused the death of nearly 3.8 million people worldwide (The John Hopkins University Database). This disease, named COVID-19, is caused by the novel coronavirus SARS-CoV-2, which was first detected in Wuhan, China (Adhikari et al., 2020). SARS-CoV-2 is a single-stranded RNA virus belonging to the *Coronaviridae* family of viruses (Yan et al., 2020). With an average diameter of 100 nm, SARS-CoV-2 possesses four structural proteins; spike, nucleoprotein, membrane, and envelope proteins. This spike protein is believed to have a binding affinity at least ten times higher than the affinity that of SARS-CoV-1, contributing to its highly contagious nature (Wrapp et al., 2020).

The main routes of transmission for SARS-CoV-2 include direct contact with infected droplets from coughing and sneezing, the surface to hand to mucus transfer, aerosol and dust inhalation, and ingestion of contaminated food and soil (Doremalen et al., 2020, Hoseinzadeh et al., 2020, Kumar et al., 2020). There is evidence indicating that SARS-CoV-2 is likely to result in enteric contagion and is found in human feces (Gu et al., 2020; Cholankeril et al., 2020). For example, two reports have indicated that SARS-CoV-2 viral RNA segments were detected in the stool of about 2% to 10% of patients with established COVID-19 (Chen et al., 2020; Wong et al., 2020). Therefore, fecal matter inputs to the environment due to wastewater discharge may increase the risk of becoming infected with SARS-CoV-2 in associated recreational waters and untreated drinking water, especially in underprivileged communities (Cahill and Morris, 2020; Arslan et al., 2020).

It has been shown that many disinfectants used for tertiary treatment of wastewater in Municipal water reclamation facilities (WRFs), including the most commonly used sodium hypochlorite, are most effective at inactivating SARS-CoV-2 viral particles, reducing the risk of contamination as previously described (Wang et al., 2020; Ahmed et al., 2021). However, monitoring the presence of SARS-CoV-2 in municipal WRF influent has been proposed as a tool for community-level outbreak detection and epidemiological study (Ahmed et al., 2020; Boogaerts et al., 2021; Westhaus et al., 2021; Kitajima et al., 2020). The de facto sewershed population includes everyone contributing to the collective wastewater at the time of sampling, even tourists, asymptomatic patients, and underserved communities (Mao et al., 2020). Asymptomatic patients are a serious concern because they can go undetected and contribute to the spread of COVID-19 among the community. The presence of asymptomatic SARS-CoV-2 infections suggests that these conditions are generally not accounted for in community-level epidemiological studies. The total number of reported cases is usually lower than the number of diseases present in the community (Gundy et al., 2009). Hence, sewage sampling at the treatment plant represents collective input of contaminants by all persons physically residing in the sewershed and provides a useful opportunity to track the number of active infections in the community along with other excellent tools such as clinical testing. Wastewater influent surveillance has proven to be a powerful tool in estimating community-level circulation of other public health-related contaminants such as narcotics, pesticides, and pharmaceuticals (Lorenzo and Pico, 2019). Several recent efforts have successfully applied this powerful tool to estimate community-based outbreaks of COVID-19 and reestablished the usefulness of wastewater-based epidemiology for surveillance and prediction of COVID-19 (Medema et al., 2020; Randazzo et al., 2020; Peccia et al., 2020a).

Wastewater-based epidemiology for COVID-19 mainly relies on detecting and quantifying any of three primary SARS-CoV-2 marker genes in community wastewater influent, N1 and N2, (Xagoraraki and O'Brien, 2020; Lu et al., 2020). The general strategy for wastewater-based epidemiology for SARS-CoV-2 is to sample the influent of wastewater treatment plants or upstream for identifying local sources when WWTPS catchments are large, extract total RNA from a known volume of influent sample, and then estimate SARS-CoV-2 gene copy numbers per mL of the sample using reverse transcriptomics coupled with reverse transcriptase quantitative PCR (RT-qPCR) (Ahmed et al., 2020). However, very few studies have examined other wastewater matrices for SARS-CoV-2, including primary clarifier solids, mixed liquor bacterial activated biomass, and anaerobically digested biosolids, otherwise known as "sludges or biosolids" (Kocamemi et al., 2020). In a typical wastewater treatment employing an activated sludge process, the incoming raw influent passes through preliminary treatment units such as course screens and grit chambers before passing on to the primary clarifiers. After that, the treated wastewater typically flows through a bioreactor. After a specific hydraulic retention time, the mixture of treated wastewater and mixed liquor sludge is taken to a gravity settler where most of the suspended biosolids settle down (Metcalf and Eddy, 2014). By nature of these settling processes, particles tend to partition into solids and settle down as well. In one study, nearly 26% of viruses examined were adsorbed to the solids portion of wastewater (Ye et al., 2016).

Although sampling raw influent for community-level surveillance of SARS-CoV-2 represents an obvious choice, the use of influent samples still presents some challenges (O'Reilly et al., 2020: Peccia et al., 2020a). In particular, the concentration of viruses from large volumes of wastewater can make sample processing difficult. Alternatively, primary or secondary sludge provides a well-mixed concentrated sample needed to extract an adequate amount of RNA for further testing (Peccia et al., 2020a), although challenges such as PCR inhibition do exist in sludge samples also. Furthermore, differences in methodologies for processing influent samples have shown variable recovery efficiencies, reducing the reproducibility of these studies' results (Ahmed et al., 2021; Ahmed et al., 2015; Ahmed et al., 2020; Pecson et al., 2021). Other studies have also shown that wastewater influent can reveal a time lag between the number of detected cases and the detection of SARS-CoV-2 gene copy numbers in influent (Weidhaas et al., 2021). However, it has been shown that some viral pathogens and SARS-related viruses can remain infectious in sewage samples for days to weeks (Wigginton et al., 2015). This suggests that SARS-CoV-2 may be detected in sludge samples even with long retention times, and therefore sludge gene copy numbers may account for a time lag (Casanova et al., 2009). The monitoring of wastewater treatment sludges could potentially provide additional tools for SARS-CoV-2 tracking in wastewater treatment plants, especially in communities with low caseloads or in periods early on in detection. Only a few previous studies have examined the relationship of SARS-CoV-2 in wastewater biosolids to sewershed disease burden. Still, they have solely focused on primary sludge and return activated sludge, completely ignoring anaerobically digested sludge (Peccia et al., 2020a; Kocamemi et al., 2020). Additionally, previous studies have not provided a clear picture of where SARS-CoV-2 viral particles and associated genetic material are removed in the wastewater treatment process before final disinfection (Kocamemi et al., 2020). Therefore, this research provides a different scenario for wastewater-based epidemiology for SARS-CoV-2 in terms of monitoring sludge samples.

This project investigated the presence and abundance of SARS-CoV-2 gene copy numbers within the influent, primary sludge, return activated sludge, and anaerobic digester sludge of municipal wastewater treatment trains varying inflow quantities and type of treatment. From this data, we determined where SARS-CoV-2 is most abundant within WRF sludges. At what point of the treatment train SARS-CoV-2 is removed before the final effluent is discharged into the environment. If sludge samples are comparable to influent samples as predictors of disease burden in a sewershed. This study's working hypothesis is that SARS-CoV-2 tend to partition into the solids phase of sludge samples and that their abundance within sludge samples will be predictive of community-level COVID-19 disease prevalence.

2. Materials and methods

2.1. Wastewater treatment plants and sampling details

Wastewater and biosolids samples were collected twice a week from seven WRFs between May 18th and July 21st of 2020, capturing a nine-week period during which national quarantine protocols had been established. Specifically, samples from the Provo City Water Reclamation (PCWRF), North Davis Sewer District (NDSD), Snyderville Basin Water Reclamation Facility-Silver Creek (SCWRF), and Snyderville Basin Water Reclamation Facility-East Canyon (ECWRF), were studied for the full nine weeks, while samples from Salt Lake City Water Reclamation Facility (SLCWRF), Timpanogas Special Services District (TSSD), and Central Valley Water Reclamation Facility (CVWRF) were collected for the last five weeks of the sampling period. The metadata and sample types for each WRF are shown in Table 1. Daily flow and solid retention time (SRT) values were determined by calculating the average for the summer sampling period. All facilities treated their wastewater using an activated sludge aeration basin system and were, therefore, able to provide both raw influents and return activated sludge (RAS) samples. As indicated in Table 1, primary clarifier sludge and anaerobically digested sludge samples were supplied by CVWRF, PCWRF, and NDWRF. SLCWRF and TSSD use industrial pretreatment processes rather than primary clarifiers. Therefore they could only provide additional digested sludge samples. Influent samples were taken as 1-L subsamples of a 24-h composite raw influent, after course screening and before the grit chamber, if any. The RAS, primary sludge, and digested sludge samples were collected as 250-mL to 1-L grab samples from the wasting lines. The locations of each WRF can be seen from the heat maps shown in Fig. 1.

2.2. Sample processing

2.2.1. Method development for liquid samples

All samples were handled according to approved protocols by the Institutional Biosafety Committee (HMR; 49 C.F.R., Parts 171–180). After the samples were collected aseptically in sterile containers by wastewater treatment plant operators, they were transferred to the University of Utah in secondary containers on ice within 4 h after collection. Before processing, all samples were incubated for 2 h at 65 °C to inactivate live viral particles. To develop a reliable method for processing all liquid samples, two related methods (Method A and Method B), were adopted from Ahmed et al. (2015), Ahmed et al. (2020), Pecson et al., (2021), and Weidhaas et al., (2021), with some variations, and were used to test the relative recovery efficiency of those samples. To make a blind comparison, we processed one set of influent samples from three different wastewater treatment plants separated geographically using the two methods above. Method A called for adjusting liquid samples to a pH of between 3.0 and 3.5 using 2.0 N hydrochloric acids. Next, a volume of 100 to 200 mL of the acidified liquid samples was filtered using a vacuum filtration through 0.22-um-pore-size cellulose electronegative filter membranes. Filter papers were then placed into a sterile 50 mL falcon tube and stored at −80 °C for long term storage until RNA extraction was performed. In the modified Method B, the fluid samples were first centrifuged at 4000 ×*g* for 20 min, and the supernatant was gently removed from the semi-solid pellet. The supernatant was then acidified to the same pH as specified in Method A and vacuum filtered on the same filter paper. The remaining semi-solid pellet was then discarded based on the assumption that most viral particles remain suspended in the liquid fraction at low centrifugation speeds. The sample processing was performed in a separate laboratory space equipped with a biosafety level 2 hood, a temperature incubator, a vacuum pump, and other necessary supplies for aseptic sample processing.

2.2.2. The effect of pH and temperature on SARs-CoV2 gene copy numbers

To study the effect of pH on SARs-CoV-2 gene copy numbers, a randomly chosen and previously heat-treated influent sample from one of the treatment plants was divided into three aliquots of 200 mL. Each aliquot was then adjusted to either a pH of 3.5 using 2.0 N hydrochloric acid or a pH of 10 using 0.5 N sodium hydroxide; no adjustment was made to one of the aliquots to serve as a control. The aliquots were then processed using Method A as described earlier, followed by RNA extraction and qPCR. Likewise, to examine the effect of temperature, another randomly chosen influent sample but not heat treated was divided into triplicate aliquots, which were then incubated at 25 °C, 35 °C, 65 °C, and 75 °C for 2 h before being processed using Method A, as described above. All of the experiments were performed as technical triplicates to obtain the average SARS-CoV-2 gene copy number per liter, or gene copies per liter (GC/L), and the corresponding standard deviation.

2.2.3. Sludge sample processing

For the RAS, primary sludge, and digested sludge samples, SARS-CoV-2 viral particles and genetic material was directly extracted from the sludge matrix without transferring them to the aqueous phase was an adjustment to the sludge processing methods described by Kocamemi et al., 2020. Biosolid samples were processed by centrifuging 50 mL of well-mixed sludge at 10,000 ×g for 2 min. The supernatant of each sludge sample was immediately decanted and stored for further processing. Multiple samples were centrifuged to obtain a final supernatant volume of 50 to 100 mL, which were then processed using the same Method A, which was used to process influent samples. The resulting solid sludge pellet was immediately stored at −80 °C for later RNA extraction. 0.5 g of sludge pallet was used to extract genetic material. Additionally, the solid sludge pellet volume was recorded, and the volatile suspended solids in the supernatant were measured using the Standard Methods as described earlier. Both values were used to calculate the final GC/L values. The gene copy numbers determined for the supernatant and solid sludge pellet were eventually combined after calculation and reported as a single value.

2.3. RNA extraction

RNA extraction was performed on both filter membranes and sludge samples manually using AllPrep Power Viral DNA/RNA kit (Qiagen, Hidden, Germany). Prior to extraction, 800 μL of solution PM1 (heated at 55 °C) and 8 μL of β-mecaptoethanol (MP Biomedicals, Irvine, CA) were added to freeze filter paper or sludge pallet, vortexed and homogenized on a bead ruptor 12 (OMNI International). After bead beating, Qiagen protocol was followed for further RNA extraction. Final purified

Table 1
Water reclamation facility metadata and sample types.

WRF	Population served	Flow (MGD)	SRT (days)	Weeks sampled	Influent	Primary sludge	RAS	Digested sludge
PCWRF	214,223	10	12	9	Yes	Yes	Yes	Yes
NDSD	227,000	21	8.0	9	Yes	Yes	Yes	Yes
SLCWRF	209,645	32	4.0	5	Yes	No	Yes	Yes
TSSD	253,098	20	8.5	5	Yes	No	Yes	Yes
CVWRF	515,494	49	7.3	5	Yes	Yes	Yes	No
SCWRF	14,000	1.2	18	9	Yes	No	Yes	No
ECWRF	16,400	3.6	18	9	Yes	No	Yes	No

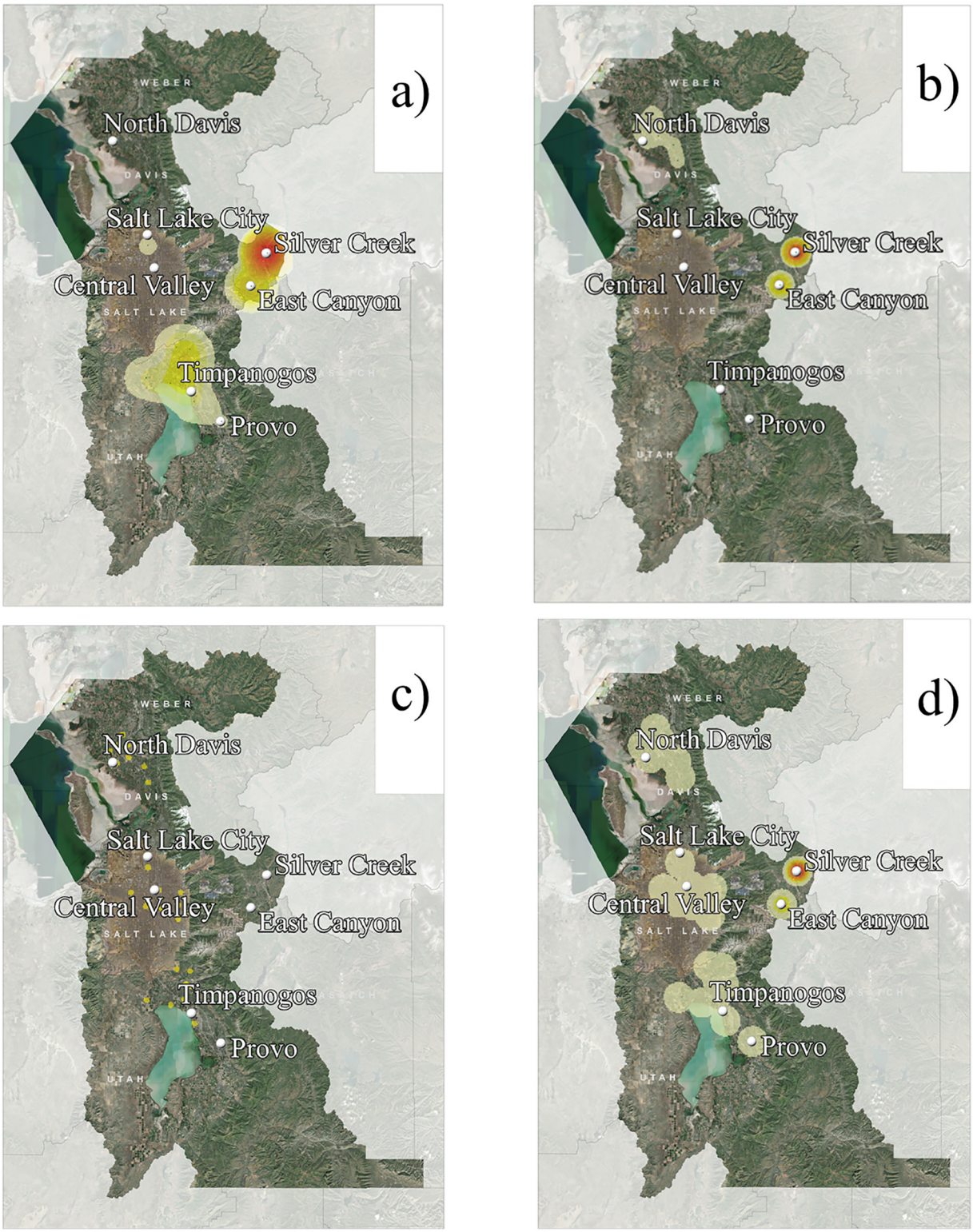

Fig. 1. a-d: The relative abundance of SARS-CoV-2 marker gene copy number per liter and spatial contribution of each sewershed for all seven WRF's for a) week 5 influent b) week 5 RAS c) week 6 influent d) week 6 RAS.

RNA was transferred to 2 mL low DNA binding tubes and stored at −80 °C until further used for reverse transcription.

2.4. Real-time quantitative polymerase chain reaction for SARS-CoV-2

For the detection and quantification of SARS-CoV-2 gene copy numbers in extracted RNA samples, reverse transcriptase quantitative polymerase chain reaction (RT-qPCR) assay with primers designed by US Centers for Disease Control and Prevention (CDC) was used. The positive control and primer-probe mixture targeting the N1 gene (CDC, 2020) used in this study were purchased from Integrated DNA Technologies (Coralville, IA, USA). The 2019-nCoV RT-qPCR assay included target N1, which was specifically designed for the detection of 2019-nCoV. The probe sequences of 2019-nCoV RT-qPCR assay N1 and the

forward primer sequence of 2019-nCoV RT-qPCR assay N2 showed high sequence homology with previous SARS coronavirus strains. For the RT-qPCR assay targeting each gene, a master mix composed of 5 μL of TaqPathTM 1-Step RT-qPCR Master Mix (ThermoFisher Scientific, USA), 8.5 μL of nucleus free water, 1.5 μL primer-probe mixture, and five μL of template RNA for a total volume of 20 uL. The thermocycler temperature conditions were initiated for 2 min at 25 °C and then 15 min at 50 °C, followed by 45 cycles of 3 s at 95 °C and 30 s at 55 °C. The 2019-nCoV Positive Control (nCoVPC) consisted of an in vitro transcribed RNA, which yielded positive results for both N1 and N2 primer-probe mixtures. For each RT-qPCR run, five sets of positive controls were used, as well as unknown samples spiked with positive controls and negative controls. All of the samples and controls were analyzed as technical triplicates. *The 95% limit of detection (95%LOD) for the N1 assay was estimated using serial dilution of N1 template in actual wastewater samples.*

The RT-qPCR assays were performed using Quantstudio™ 3 Real-Time PCR machine (Thermofisher Scientific, USA). A five-point calibration curve was made using known gene stock solutions purchased from Integrated DNA Technologies (Coralville, IA, USA). The amplification efficiencies (E) were calculated based on the equation: $E = 10^{(-1/\text{slope})} - 1$. Matrix spike tests were performed to evaluate the RT-qPCR efficiency by spiking a known volume of water with a known gene copy numbers of SARs-CoV-2 N1 gene. The water used was collected from lab scale biological reactor receiving synthetic feed.

All RT-qPCR reactions were performed in triplicate and any calibration curve with an R^2 value less than 0.98 was discarded. Apart from positive and negative controls in each qPCR 96-well plates, other quality controls were also performed. For each WRF, a raw influent sample was spiked with a known number of N1 genes from the stock solution and the spiked sample was treated as unknown to evaluate matric effect on PCR amplification efficiency. As suggested in Ahmed et al. (2020), RNA extraction and RT-qPCR were conducted in separate laboratories to avoid any potential RT-qPCR contamination. For final gene copy number calculation, C_T method was used, in which case amplification efficiencies between 90% and 100% were considered for each sample analyzed.

2.5. Public health data and KDE heat mapping

Service district maps were obtained for each district managing the seven WRFs that were examined in this study. The Utah Department of Health provided public health data related to positive COVID-19 cases. The number of daily cases were simply positive COVID-19 cases recorded each day, with less than five positive COVID-19 cases recorded as "<5" to protect individual anonymity. The daily infection rate was recorded as the number of cases per day per100K people served, which was based on the population of each district. Weekly cases were calculated as the sum of daily cases for the corresponding sampling week, while average daily cases were calculated as the average number of cases per day for the corresponding sampling week. Each of these parameters were then tested in subsequent statistical analyses, as described later.

The geographical distribution and spatial contribution of the sewershed districts to the density of SARS-CoV-2 gene copy numbers for influent and RAS samples were mapped using a kernel density estimation (KDE) algorithm and GIS software. Kernel density estimation quartic biweight kernel (KDE) is a global, descriptive statistical algorithm that uses a spatial, discrete histogram to show a smoothed distribution of data over a surface area (Alygizakis, 2016; Sinclair et al., 2019). KDE is used in public health to research disease outbreaks and spread (Dallas et al., 2019; Sinclair et al., 2019). It is calculated by using weights and distances of all data points. A smoothed surface is fitted over each weighted data point (Huang et al., 2019). The surface's value is densest at the data points with the highest weighted values and lowest with the lowest weighted values and decreases with distance until it reaches a search radius of 0 from each kernel function (WU and Man-qi, 2018). The concept of weighting the distances of our observations from a particular point, x, can be expressed mathematically as shown in Equation 1:

$$\widehat{f}(x) = \sum_{observations} K\left(\frac{x - observation}{bandwidth}\right) \quad (1)$$

The contribution of data point x(i) to the estimate at some point x depends on the distance between x(i) and x. Estimate function is x. Kernel function is K. Bandwidth is h.

Calculation for kernel density estimation rate is expressed as shown in Equation 1:

$$(\textbf{Wastewater facility}/\textbf{total population})/\textbf{wastewater participating cities}) = \textbf{Kernel Density Estimation Rate per Metric Measured} \quad (2)$$

KDE was used in this study to identify the location of the viral load from the RT-qPCR results. Seven wastewater facilities that are placed in Figs. 1a-d have contributing populations to the viral load results. The KDE as the density load by wastewater facility was divided by population and number of cities. The results are a series of heat maps for each week of testing, each facility and population describes the spatial impact and distribution of SARS-CoV-2 gene copy numbers.

2.6. Data normalization and statistical analysis

As detailed in Ahmed et al., 2020, a recovery ratio of 26% was used to estimate the original GC/L recovered by membrane filtration for influent and sludge supernatant samples (Ahmed et al., 2020). To calculate averages and standard deviations of SARS-CoV-2 of GC/L, any non-detect samples were assumed to be equal to zero; however, 100% of influent and sludge samples had an associated detected value. In the analysis of public health data, days with less than five new daily cases were estimated as half the maximum number of cases in that range. Although the calculation of GC/L was sufficient to make comparisons between treatment train processes within each WRF, to make comparisons between each WRF the raw data was normalized to account for average daily flow and population size by converting GC/L to million viral gene copies per capita per day (MVGC/capita/day) using Eq. 3:

MVGC = (gene copies / L wastewater) × (L wastewater influent / day) × (1 / population) (Ahmed et al., 2015).

Nonparametric regressions of SARS-CoV-2 log gene copy number over time were performed using *loess* in R version 4.0.3, which performs local least-squares to form smoothed estimates. To evaluate the significance of the differences found between SARS-CoV-2 gene copy numbers in influent and sludge samples, one-way ANOVA tests, and Tukey's HSD tests were performed on each sample type WRF, which represents the entire sampling period using RStudio software. The bar graphs were visualized in Origin, and the box plots were created using RStudio software. To determine if there were any significant correlations between gene copy numbers and positive COVID-19 cases in influent and RAS, multiple generalized linear regression analyses were performed using each public health parameter for both raw and normalized data, as described above, using R Studio software. Linear mixed-effects models (LME) were also performed in R Studio to determine whether SARS-CoV-2 gene copy numbers measured in primary sludge could predict the number of COVID-19 cases for that day, as well as cases with a one- and two-week time lag. This model allowed for random intercepts, which represent different baseline levels of infection for each sewer shed. The model was considered statistically significant if the t-value is approximately equal to two ($t \approx 2.00 \pm 0.30$). All other analyses were considered significant if they resulted in a *p*-value less than 0.05 (p-value <0.05).

3. Results

3.1. Method development and effect of pH and temperature

In matrix spiked samples, as such, we did not see any inhibition, and the gene copy numbers were in the proximity of expected gene copy numbers within a range of 95% to 105%. The three WRFs that provided influent samples that were tested in this experiment were Salt Lake City WRF (SLCWRF), Timpanogas Sewage District (TSSD), and Central Valley Water Reclamation Facility (CVWRF). The average SARS-CoV-2 GC/L for these WRF samples were $5.06 \times 10^4 \pm 1.14 \times 10^3$, $3.95 \times 10^4 \pm 9.70 \times 10^3$, and $7.57 \times 10^4 \pm 4.35 \times 10^3$, respectively, using Method A. For Method B, these same influent samples' results were as follows: $2.4 \times 10^4 \pm 0.64 \times 10^4$, $1.34 \times 10^4 \pm 1.31 \times 10^3$, and $4.4 \times 10^4 \pm 1.22 \times 10^4$, in the same order of WRF as described above. Hence, Method A produced significantly higher SARS-CoV-2 GC/L than using Method B (p-value <0.05). Therefore, for all further sample processing, Method A was employed.

The effects of different pH and temperatures on the relative recovery efficiency of SARS-CoV-2 viral particles and marker genes using Method A were also evaluated. Standard handling procedures require that samples need to be heat-treated for 2 h at 65 °C, and traditional influent processing methods require that the sample be acidified to a pH of approximately 3.5. It was unclear how different environmental conditions might affect the efficacy of the extraction method. The results for influent samples heated to 25 °C and 35 °C showed that SARS-CoV-2 gene copy numbers were $1.05 \times 10^4 \pm 0.87 \times 10^3$ and $1.14 \times 10^4 \pm 0.78 \times 10^3$ GC/L, respectively, and were not significantly different. The samples heated to 65 °C exhibited significantly lower gene copy numbers than the 25 °C and 35 °C samples, with an average SARS-CoV-2 gene copy number of $2.09 \times 10^2 \pm 0.75 \times 10^2$. At an incubation temperature of 75 °C, gene copy numbers were not detected, most likely due to the viral capsid's denaturation from heat damage (Qui, 2012). The influent samples' results treated to a pH of 3.5 and 7.5 exhibited gene copy numbers of $2.15 \times 10^4 \pm 0.99 \times 10^4$ and $2.72 \times 10^4 \pm 1.18 \times 10^3$ GC/L, respectively. A one-way ANOVA test shows that the difference in gene copy number between these two treatments was not significantly different. However, all samples treated to a pH of 10 resulted in a non-detect gene copy number for all samples tested, resulting in a substantially lower recovery efficiency at a basic, rather than neutral or acidic, pH value.

3.2. Prevalence of SARS-CoV-2 in WRF influent and sludges

All seven of the WRFs were sampled for both influent and RAS, four of which (PCWRF, NDWRF, CVWRF, SLCWRF) were studied for the full nine weeks of the study period, while three were studied for the final five weeks (SLCWRF, ECWRF, SCVWRF). All of the influent and RAS samples showed 100% positive hits for SARS-CoV-2 gene copy numbers. Weekly datasets that included enough sampling points to generate a KDE heat map were weeks 1, 4, 5, and 6. Of these four weeks, KDE heat maps were created for weeks that included sampling events for all seven WRFs, weeks 5 and 6. Therefore, Figs. 1a-d show the locations of each WRF and the detected relative viral load estimation calculation outputs by kernel density estimation (KDE) per-unit-area for influent and RAS at week five and week 6. The unit area size indicates the amount of geographic area that contributes waste to the wastewater treatment facilities, including 30 different cities. The magnitude of the viral load is represented by the color gradient, with red being associated with higher loads concentrated at the confluence point: the wastewater facility while expanding out from orange and yellow through portions, is associated with the central city populations contributing to the viral load. The influent and RAS heat maps for weeks 5 and 6 show distinct changes in the viral load distribution. The week influent 5 KDE heat map (Fig. 1a) indicates that most of the total SARS-CoV-2 gene copy numbers were contributed by the Park City area, with high viral loads centered around SCWRF well as much of South Salt Lake and the northern section of Utah County. However, the week six influent KDE heat map (Fig. 1c) shows that total viral load lessened drastically across the region and became more evenly distributed, with contributions coming mostly from outlying towns surrounding major cities. The week 5 RAS KDE heat map (Fig. 1b) shows that viral load reflected the trends seen in the influent for that week, with the majority of the total contributed by the Park City area; however, NDSD contributed the other portion of the total rather than TSSD and PCWRF. However, by week 6 (Fig. 1d), the viral load increases overall and becomes evenly distributed across the region, reflecting the influent gene copy numbers' trend for that week.

The WRFs that were additionally sampled for primary and digested sludge included PCWRF, NDWRF, CVWRF, SLCWRF, and TSSD. Overall trends in SARS-CoV-2 gene copy numbers over the sampling period for each sample type are shown in Supplementary Fig. S1a-d. The primary and digested sludge samples also exhibited 100% positive hits for SARS-Cov-2 gene copy numbers. A Tukey's HSD analysis revealed that, for these five WRFs, only TSSD showed no significant differences (p-value <0.05) between any sample type for all combined sludge data values, and therefore was not visualized in Figs. 2a-d or Supplementary Fig. S2a-d. Additionally, only one digested sludge sample was obtained for CVWRF. Therefore this data point was treated as an outlier and removed from further downstream analyses. Overall, Figs. 2a-d show that the distribution of SARS-CoV-2 gene copy numbers between sample types was consistent over time for June and July and between the remaining four WRFs. SARS-CoV-2 gene copy numbers were highest in primary sludge (1.0×10^5 to 1.0×10^6 GC/L), followed by influent (1.0×10^4 to 1.0×10^5 GC/L). RAS and digested sludge showed similar gene copy numbers with each other, and both were magnitudes lower than primary sludge (1.0×10^3 to 1.0×10^4 GC/L). Although CVWRF samples did not include digested sludge and SLCWRF samples did not include primary sludge, the same distribution held for the remaining sludge samples of these two WRFs.

The results of Tukey's HSD analysis on combined data are summarized in Table 2. It was found that for PCWRF, primary sludge had significantly greater gene copy numbers than other sample types. NDWRF showed a similar significant difference in gene copy number between primary sludge and other sample types, but with p-values slightly above 0.05. Similar to PCWRF sludges, the abundance of SARS-CoV-2 gene copy numbers in CVWRF primary sludge samples was significantly higher than influent and RAS. However, for SLCWRF, only influent was significantly higher than RAS, but not digested sludge samples. Fig. 3 shows the results of multiple linear regression analysis for all influent and RAS values in terms of gene copies per liter. This analysis showed that only ECWRF ($R^2 = 0.775$, p-value = 0.009) and SCWRF ($R^2 = 0.681$, p-value = 0.007), which do not possess primary clarifiers, gene copy numbers increased significantly in RAS with increased inputs from the influent. For the other five WRFs that do possess either primary clarifiers or industrial pretreatment processes, SARS-CoV-2 gene copy numbers in RAS did not increase significantly, regardless of the influent's inputs.

3.3. Relationship of SARS-CoV-2 to community infection rates

Supplementary Fig. S3a&b depict the linear regression analysis results between gene copy number per liter (GC/L) and million viral gene copies per capita per day (MVGC/capita/day) for influent and RAS. The results showed strong significant positive correlations (p-value = 1.1×10^{-15}, 2.0×10^{-16}) for influent and RAS, respectively. The average number of SARS-CoV-2 gene copies per liter and MVGC per capita per day in influent and RAS and the daily rate of COVID-19 cases for each WRF are summarized in Table 3. In summary, TSSD had the highest average GC/L in influent while ECWRF had the lowest, and SCWRF had the highest average in RAS, while SLCWRF had the lowest. After normalization for the population size of the sewershed and daily

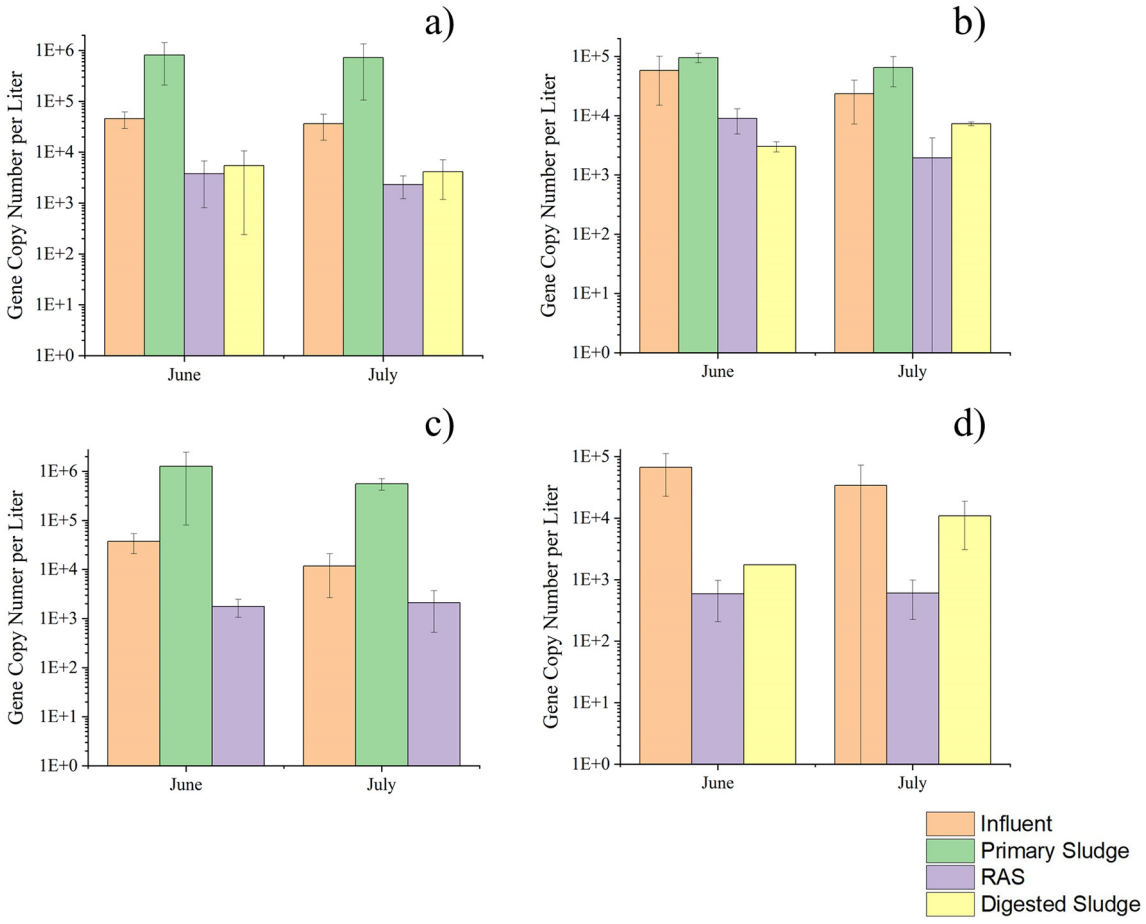

Fig. 2. a-d. Average SARS-CoV-2 marker gene copy number per liter for both June and July influent, primary sludge, RAS, and digested sludge for: a) PCWRF b) NDSD c) CVWRF d) SLCWRF.

average flow rate, SLCWRF had the highest average MVGC per capita per day in influent, while PCWRF had the lowest. However, Table 3 shows that the RAS data normalization did not change which WRF had the highest average gene copy number, which remained as SCWRF as the highest and SLCWRF as the lowest.

Figs. 4a-d show the average and standard deviation of SARS-CoV-2 GC/L in influent and RAS and daily and weekly COVID-19 cases for PWRF, NDSD, SCWRF, and ECWRF over nine weeks. Figs. 4e-g show the influent and RAS gene copy number data for SLCWRF, TSSD, and CVWRF, which were sampled for the remaining five weeks of the study period. PCWRF and SCWRF showed relatively consistent SARS-SoV-2 gene copy numbers in influent and RAS over time, ranging in the magnitude of two log, while NDSD and ECWRF showed more significant variability from week to week, going between 1.0×10^2 to 1.0×10^5 GC/L. Figs. 5a-e show the average and standard deviation of gene copy numbers of primary and digested sludge overlaid with daily and weekly COVID-19 cases. Gene copy numbers for both sludge types remained within a range of one log gene copy number, except for PCWRF digested sludge, which varied within a range of 1.0×10^2 and 1.0×10^4 GC/L. Overall, while positive COVID-19 cases increased significantly in most sewersheds, the gene copy number for influent and sludge samples remained relatively stable over the sampling period, with a few exceptions.

Multiple linear regression analyses were performed between each public health parameter, including daily, weekly, and daily rate of COVID-19 cases, as well as for both the raw (GC/L) and normalized gene copy number (MVGC/capita/day) data for influent and RAS samples at each WRF. Of the seven WRFs, as seen in Supplementary Fig. S4 a&b, only ECWRF exhibited a positive correlation between the influent gene copies per liter and the daily number of COVID-19 cases ($R^2 = 0.561$, p-value $= 0.0322$), and between RAS gene copies per liter and the weekly number of COVID-19 cases ($R^2 = 0.449$, p-value $= 0.0597$). Additionally, linear mixed-effects (LME) models that use random intercepts to represent differing baseline levels of COVID-19 cases were created to predict the daily rate of cases using primary sludge (Figs. 6a&b) gene copy number per liter data. This model could predict the daily rate for PCWRF, NDSD, and CVWRF sewersheds for the current sampling week and the following sampling week ($t = 2.279$ and $t = 2.122$, respectively). Similarly, an LME model predicted the daily rate of cases for PCWRF, NDSD, and TSSD using digested sludge data (Fig. 6c) in two weeks ($t = 2.01$).

Table 2
Significance of differences in gene copy number between different sludge sample types for PCWRF, NDWRF, CVWRF, and SLCWRF. (Note: * refers to significant difference; ** refers to highly significant difference)

Significance of relationship	PCWRF	NDWRF	CVWRF	SLCWRF	TSSD
Primary - Influent	0.000253**	0.205	0.0298*	X	X
RAS - Influent	0.992	0.923	0.991	0.0296*	0.233
Digested - Influent	0.996	0.671	X	0.116	0.181
RAS - Primary	0.000139**	0.0674*	0.0165*	X	X
Digested - Primary	0.000839**	0.0593*	X	X	X
Digested - RAS	0.999	0.903	X	0.862	0.984

4. Discussion

4.1. The relative recovery efficiency of SARS-CoV-2 genes

In this study, two methodologies and two environmental parameters were evaluated for their effect on the relative recovery efficiency

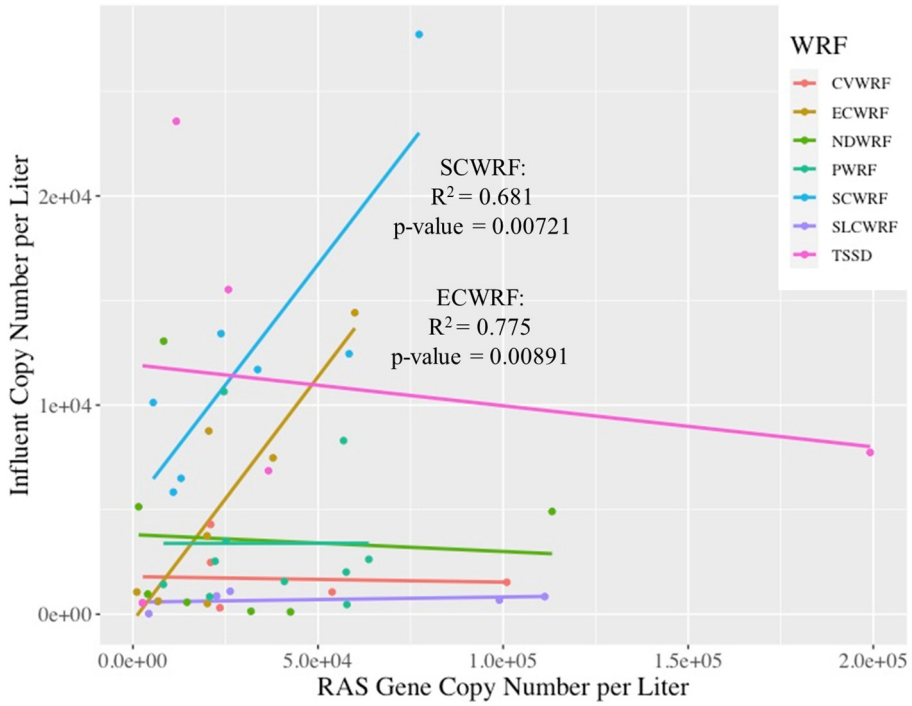

Fig. 3. Multiple linear regression analyses between influent and RAS MVGC per capita per day for each WRF. Only SCWRF and ECWRF, which do not possess primary clarifiers or industrial pretreatment processes, showed significant correlations.

of SARS-CoV-2 gene copy number for influent wastewater samples based on the methods detailed in Ahmed et al. (2015), Ahmed et al. (2020), Pecson et al. (2021), and Weidhaas et al. (2021). Overall, Method A produced significantly greater gene copy numbers than Method B, which included the quantification of SARS-CoV-2 gene copy partitioned to total suspended solids. However, the recovery of SARS-CoV-2 gene copy numbers by both methods produced results within one-log gene copy number of one another. These results agree with the findings of Pecson et al. (2021), where 80% of the results from 36 different methodologies fell within one-log gene copy number of each other. Considering the results from this study and those from Pecson et al. (2021), it remains unclear whether SARS-CoV-2 partitioned into suspended solids should be regarded as negligible because method reproducibility is within one-log gene copy number.

Our research further elucidated how variations in pH and temperature would impact the relative recovery efficiency of SARS-CoV-2 gene copy numbers influent samples. The results showed that heat inactivation at 65 °C significantly decreased the relative recovery efficiency by over one-log gene copy numbers compared to samples left at room temperature (25 °C) and slightly above (35 °C). At 75 °C, no gene copy numbers were detected all. None of these samples were initially treated at 65 °C. Therefore, the reduction in recovery efficiency due to heat inactivation at 65 °C may be an essential consideration in calculating the final SARS-CoV-2 gene copy number per liter recovered from the influent. As a result, it is strongly recommended that samples should not be heat inactivated at 65 °C before processing for actual quantification of SARS-CoV-2. In contrast to these results, the pH experiments show that acidification from a neutral pH of 7.5 to an acidic pH of 3.5 did not significantly differ in SARS-CoV-2 gene copy numbers. However,

Table 3
Average and (± standard deviation) of influent and RAS gene copies per liter (GC/L), million viral gene copies per capita per day (MVGC/capita/day), and the daily rate (daily cases/100 K population) of COVID-19 cases. Highest averages are highlighted in orange, lowest in blue.

WRF	Influent GC/L	RAS GC/L	Influent MVGC/cap/d	RAS MVGC/cap/d	Daily Cases/100K
ECWRF	2.38E+04 (1.83E+04)	5.21E+03 (4.30E+03)	2.67E+01 (2.74E+01)	4.33E+00 (3.57E+00)	10.3 (± 17.5)
SCWRF	2.56E+04 (2.49E+04)	1.59E+04 (1.03E+04)	1.49E+01 (1.45E+01)	5.32E+00 (3.45E+00)	10.1 (± 32.1)
PCWRF	3.78E+04 (1.89E+04)	3.28E+03 (3.07E+03)	1.09E+01 (6.67E+00)	5.96E-01 (5.59E-01)	18.2 (7.57)
NDSD	3.38E+04 (3.28E+04)	3.11E+03 (4.25E+03)	2.04E+01 (1.98E+01)	9.62E-01 (1.44E+00)	10.0 (± 6.64)
CVWRF	3.72E+04 (3.23E+04)	1.70E+03 (1.36E+03)	2.37E+01 (2.06E+01)	6.24E-01 (4.99E-01)	12.5 (± 12.0)
SLCWRF	4.50E+04 (4.34E+04)	6.89E+02 (3.33E+02)	4.53E+01 (4.36E+01)	3.98E-01 (1.92E-01)	17.0 (± 8.33)
TSSD	4.60E+04 (6.97E+04)	9.45E+03 (7.89E+03)	2.35E+01 (3.55E+01)	2.77E+00 (2.31E+00)	7.94 (± 4.71)

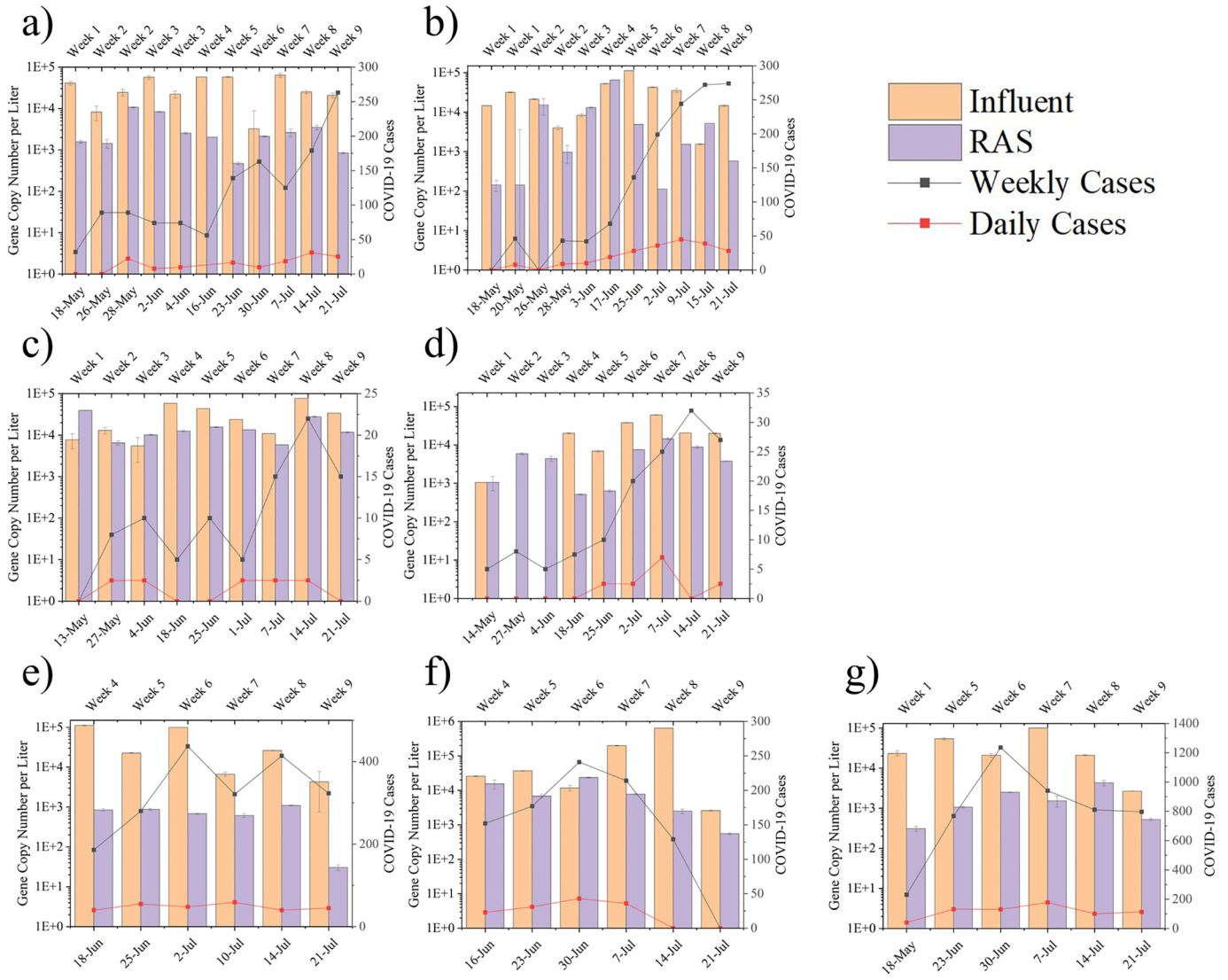

Fig. 4. a-g. The average SARS-CoV-2 marker gene copy number per liter for influent and RAS over the course of nine weeks of the summer 2020. Overlaid line graphs show the average number of COVID-19 cases in terms of total daily and weekly cases. Water Reclamation Facilities are ordered as follows: a) PCWRF b) NDSD c) SCWRF d) ECWRF e) SLCWRF f) TSSD g) CVWRF.

increasing the pH of influent samples to 10 resulted in non-detection of any gene copy numbers for all trials tested. Therefore, acidification of samples does not produce a significant loss in SARS-CoV-2 gene copy numbers and can be neglected in the final calculation of SARS-CoV-2 gene copy numbers, as long as the original influent sample has an initial neutral pH. It may be necessary to check the pH of samples before acidifying them to determine whether the baseline pH is more basic and, therefore, affect the final SARS-CoV-2 gene copy numbers.

4.2. WRF Sludges Harbor SARS-CoV-2 genes

Overall, SARS-CoV-2 gene copy numbers were detected in 100% of influent and RAS samples taken throughout the sampling period for all seven WRFs. Of the five WRFs that additionally were sampled for primary sludge and anaerobically digested sludge, 100% of those samples also detected SARS-CoV-2 gene copy numbers. The abundance of SARS-CoV-2 gene copies was similarly distributed between sample types for all WRFs and for both June and July. Despite the dissimilarities in size, flow, configuration, and sewershed population of each WRF, the data indicates a strong overall trend in the relative abundance of SARS-CoV-2 gene copy numbers throughout the general wastewater treatment process. Each of these treatment train processes is instrumental in removing different contaminants and work by other mechanisms. Primary clarifiers reduce the amount of inorganic and volatile suspended solids through physical sedimentation. However, some WRFs introduce chemical coagulants that increase flocculation to increase settling velocity and removal efficiency. Activated sludge systems work through biological processes, where leftover organic suspended solids and other dissolved contaminants are consumed as a substrate by bacteria, metabolizing them into biomass and constituent byproducts. Anaerobic digestion is also often employed to reduce the amount of biomass created in the activated sludge process to minimize waste and lessen the number of pathogens existing within the mixed liquor suspended solids (Metcalf and Eddy, 2014).

In this study, primary sludge samples contained significantly greater SARS-CoV-2 gene copy numbers than RAS and digested sludge samples for all WRFs with primary clarifier systems. These primary sludge samples accumulated one to two log gene copy numbers from influent, most likely due to the partitioning of viral particles and genetic material into biosolids, followed by the concentration and sedimentation of total suspended solids (Ye et al., 2016). There was then a significant reduction in gene copy numbers in RAS samples relative to primary sludge and influent samples. This reduction is most likely due to the removal of suspended solids by the primary clarifiers preceding the activated

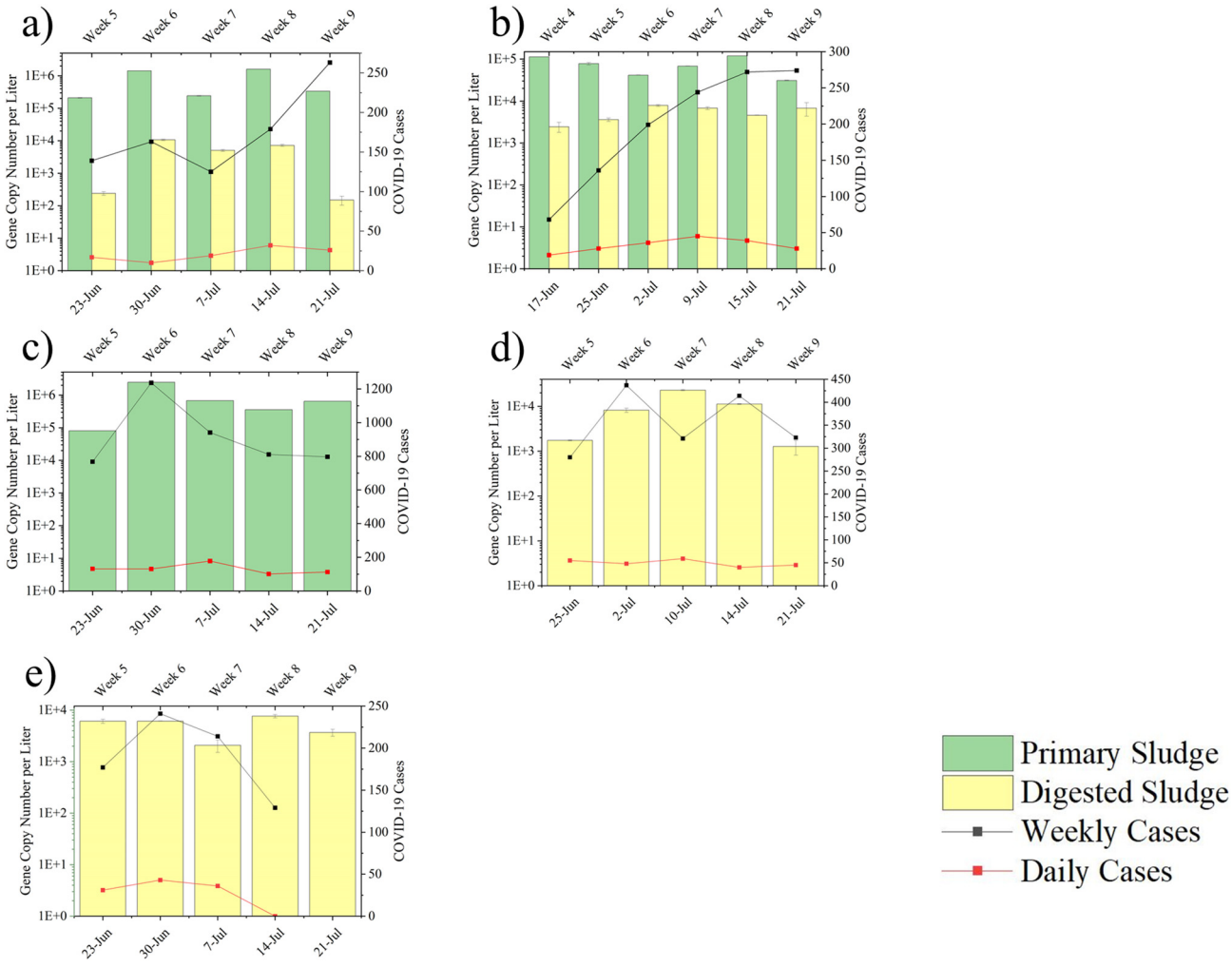

Fig. 5. a-e. The average SARS-CoV-2 marker gene copy number per liter for primary and digested sludge over the course of the sampling period. Overlaid line graphs are the average number of COVID-19 cases in terms of total daily and weekly cases. Water Reclamation Facilities are ordered as follows: a) PCWRF b) NDSD c) CVWRF d) SLCWRF e) TSSD.

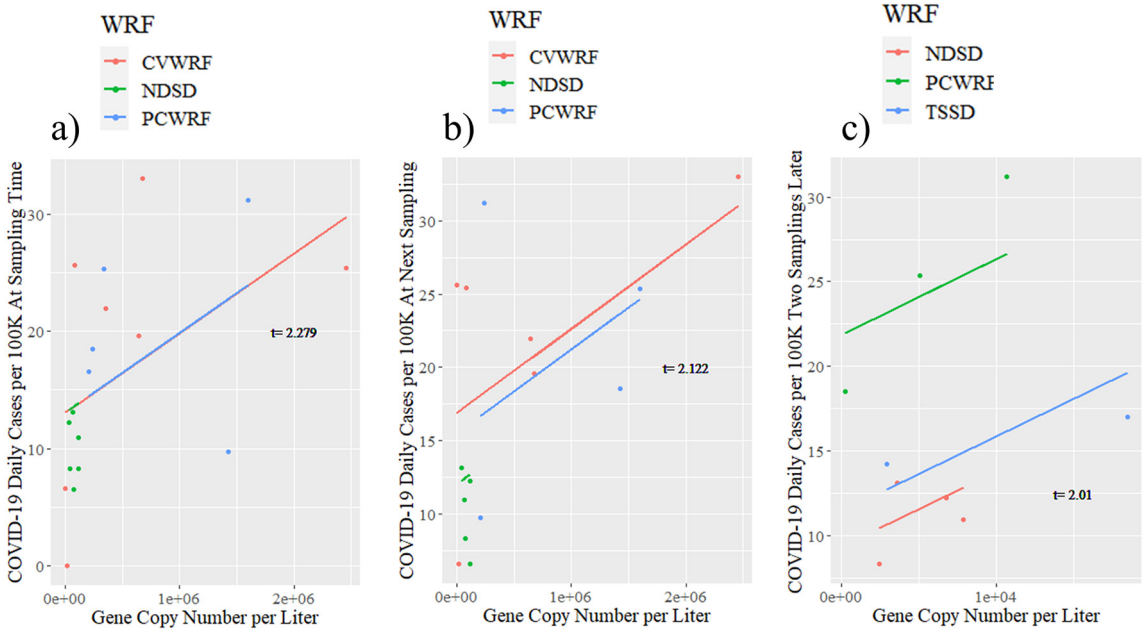

Fig. 6. a-c. Significant results of linear mixed effects models with randomized intercepts for a) primary sludge gene copy number and the daily rate of cases that week, b) primary sludge gene copy number and the daily rate of cases in one week, and (c) digested sludge gene copy number and the daily rate of cases in two weeks ($t \approx 2.00$).

sludge system rather than the activated sludge system's environmental conditions (Hata et al., 2013). After performing a generalized linear regression analysis of SARS-CoV-2 gene copy number per liter between influent and RAS for all WRFs (Fig. 3), it was found that only ECWRF and SCWRF showed significant positive correlations. These two WRFs have the smallest sewershed populations and the lowest daily flows in a million gallons per day (MGD). They, therefore, do not employ primary clarifiers in their wastewater treatment train. Within this context, the data indicates that some pretreatment process does not remove SARS-CoV-2 particles and genetic material in influent before entering the activated sludge system. Thus, the gene copy numbers in influent directly correlate with the gene copy numbers in RAS due to the lack of an intermittent removal step.

In contrast, the gene copy number in RAS for PCWRF, NDSD, and CVWRF did not increase, regardless of the inputs coming from the influent, most likely due to the action of their primary clarifiers. Additionally, influent and RAS gene copy numbers for TSSD and SLCWRF did not show a significant correlation. Although they do not possess primary clarifiers, the influent from these WRFs undergo other pretreatment processes to treat industrial wastewater. These processes likely remove SARS-CoV-2 gene copies before entering their activated sludge system (Venugopal et al., 2020).

Interestingly, was no significant difference in gene copy numbers between RAS and digested sludge samples; in fact, there was a slight increase in gene copy numbers in digested sludge for PCWRF, NDSD, and SLCWRF. Therefore, this data indicates that SARS-CoV-2 viral particles and genetic material may continue to partition into the solids fraction of samples and are not inactivated or destroyed by the mesophilic, anaerobic conditions the digester (Zhang et al., 2017). Research from previous studies and the results from the recovery experiments indicate that high temperatures (>65 °C) and pH values (pH = 10) are required to reduce SARS-CoV-2 gene copy numbers and destroy their associated genetic material (Gundy et al., 2009). The environmental conditions within the anaerobic digester, most of which typically operate at an approximate temperature of 37 °C and a pH between 6.8 and 7.2, are therefore not sufficient to destroy SARs-CoV-2 viral particles or their marker genes (Wu et al., 2006; Cioabla et al., 2012). Other studies have shown that viral pathogens tend to have a greater ability to survive the anaerobic digester process than bacterial pathogens, which may introduce risks in the downstream processing and application of biosolids (Corpuz et al., 2020). It is worth further investigation to determine whether the SARS-CoV-2 gene copy numbers found in these samples belong to intact virus-like-particles or are free-floating genetic material. As viral particles, the presence of SARS-CoV-2 gene copy numbers in sludge samples may pose a risk for workers involved in any aspect of wastewater treatment getting infected with this deadly virus; as genetic material, the dissemination of virulence genes through horizontal gene transfer could increase the pathogenicity of downstream microbial communities, such as in agricultural settings where biosolids are used as fertilizer (Bogler et al., 2020; Tozzoli et al., 2017).

In total, these data support the idea that **primary sedimentation is the most effective treatment process in the removal of SARS-CoV-2 in wastewater treatment.** The data in Figs. 2a-d show that over 99.9% of SARS-CoV-2 gene copies per liter in influent are removed after the primary clarifier stage, likely through the partitioning of viral particles and genetic material into suspended solids, followed by concentration, sedimentation, and subsequent removal from the treatment train. This is the first study of its kind also to discover that a significant amount of SARS-CoV-2 gene copies are also present in anaerobic digester sludge. Only a few other studies have examined the prevalence of SARS-CoV-2 genetic material found in some, but not all, sludge sample types in a typical wastewater treatment process (Kocamemi et al., 2020; Peccia et al., 2020a). These observations have important implications for understanding how preliminary wastewater treatment processes reduce SARS-CoV-2 viral particles and genetic material from wastewater before final disinfection. The sorption of SARS-CoV-2 to biosolids during primary clarification also has implications for influent processing methods. Viral particles are less than 0.1 μm in diameter. Many SARS-CoV-2 concentration methods assume that most particles will remain suspended in the liquid fraction of samples after centrifugation (La Rosa et al., 2020). However, the results from this study indicate that a significant portion of viral particles aggregates with other suspended materials, even under typical settling velocities. Therefore, it is advised that suspended solids' contribution to total SARS-CoV-2 gene copy number found in influent should not be ignored. Processing sludge samples may be more efficient and effective at producing reproducible results.

4.3. Influent and Sludges as indicators of sewershed disease burden

Overall, most of the SARS-CoV-2 gene copy numbers found in influent and sludge samples did not significantly correlate, using generalized linear regression analyses and linear mixed-effects models. Although the number of positive COVID-19 cases increased significantly over time, the amount of SARS-CoV-2 gene copies found in influent samples remained highly variable over the sampling period for most WRFs. The number of reported COVID-19 cases was analyzed in daily cases, weekly cases, and the daily rate of cases per 100 K persons. In contrast, SARS-CoV-2 gene copy numbers were analyzed using gene copies per liter (GC/L) and million viral gene copies per capita per day (MVGC/capita/day). This data was statistically analyzed for correlations between these data sets using generalized linear regressions and linear mixed-effects models, which allow random intercepts to represent different baseline number of COVID-19 cases. Overall, the influent data produced the least number of significant correlations; only ECWRF influent gene copy numbers (in terms of both GC/L and MVGC/capita/day) correlated with public health data as daily COVID-19 cases.

Interestingly, no relationships between disease burden and gene copy number were found for SCWRF, similar to treatment configuration. It serves a similar sewershed in terms of population and demographics as ECWRF. These results agree with the findings of Weidhaas et al. (2021). This study examined SARS-CoV-2 data obtained from examining influent samples in an overlapping geographic region of Utah for an earlier period of the pandemic. Of all the WRFs that were sampled, ECWRF was one of the few treatment facilities that exhibited a significant correlation between SARS-CoV-2 gene copy numbers in influent and daily reported cases of COVID-19, and only after accounting for a one-week time lag. Some other monitoring efforts have also failed to consistently predict the number of positive points, especially in high-prevalence areas, and using simple mathematical models (Kitajima et al., 2020). More success has been had in low-prevalence areas, similar to the ECWRF sewershed, where SARS-CoV-2 gene copy numbers in influent could accurately predict the increase in cases over two weeks (Randazzo et al., 2020).

However, the results from this study show that relatively simple analyses of the gene copy number in sludge samples had greater predictive power than data obtained from influent samples, and that they also account for a time-lag in the onset of illness and the positive result of a COVID-19 test. It was found that SARS-CoV-2 gene copy numbers from ECWRF RAS samples positively correlated with the weekly, rather than daily, number of cases. It was also found that SARS-CoV-2 gene copies found in primary sludge significantly predicted the weekly number of cases of the current week and with a one-week lag, for all three WRFs that possessed primary clarifier systems (PCWRF, NDSD, and CVWRF). Additionally, digested sludge gene copy numbers significantly predicted the weekly number of cases with a two-week lag for all three WRFs that possessed anaerobic digesters (PCWRF, NDSD, and TSSD). In total, the results from the linear regression analyses and linear mixed effects models indicate three major points: that (Abboud et al., 2020) the analysis of influent samples may be better suited to provide daily estimations of COVID-19 cases in low-prevalence sewersheds, (Adhikari et al., 2020) that primary and digested sludge samples may provide

greater predictive power of disease burden than influent samples, and (Ahmed et al., 2015) that sludge samples of any type may account for the time-lag between the onset of illness and the positive result of a COVID-19 test due to longer retention times within the WRF. These findings agree with a recent study that proved **SARS-CoV-2 gene copy numbers enumerated from primary sludge is a better predictor of COVID-19 cases than influent data** (Peccia et al., 2020b). Additionally, there still remains some difficulty and uncertainty in influent processing methods that may make sludge sample processing a more attractive option for wastewater epidemiology (Pecson et al., 2021). Therefore, this research provides multiple reasons why sludge samples, particularly primary sludge, may be a better matrix than influent samples in wastewater surveillance of SARS-CoV-2.

4.4. Implications and conclusions

According to the CDC and published reports**,** the SARS-CoV-2 virus is present in human feces by infected individuals (CDC, 2020). Although it has a low potential to be infectious through fecal contamination, it can be found in sewage due to viral shedding of SARS-CoV-2 from the fecal matter of all infected individuals within a particular sewershed (Gu et al., 2020; Cholankeril et al., 2020). Other constituents related to public health, such as narcotics and pharmaceuticals, have been monitored through the examination of influent samples in wastewater tracking epidemiology (Lorenzo and Pico, 2019). However, current methods for the analysis of influent samples can be difficult and time consuming, are so varied that they are difficult to reproduce, and ultimately do not always provide the predictive power needed for accurate wastewater tracking (Pecson et al., 2021; Sims and Kasprzyk-Hordern, 2020). The analysis of sludge samples has therefore been suggested as an alternative matrix in the investigation of SARS-CoV-2 (Peccia et al., 2020b). Additionally, very few studies have examined the removal of SARS-CoV-2 throughout various wastewater treatment processes (Hata et al., 2013). Therefore, this study examined the prevalence and abundance of SARS-CoV-2 gene copy numbers in influent and wastewater sludges, and its relationship to reported cases of COVID-19. Strategic sampling, processing, and statistical analysis of SARS-CoV-2 gene copies in samples collected from seven water reclamation facilities has yielded insight into the movement and removal of SARS-CoV-2 through the general wastewater treatment train. The data from this study indicates that sedimentation by primary clarifiers performs more action in removing SARS-CoV-2 from wastewater influent than activated sludge systems and anaerobic digesters. The data also indicates that sludge samples have greater predictive power of COVID-19 cases than data obtained from influent samples. Studies have shown that most disinfection methods are able to effectively remove SARS-CoV-2 gene copies from final effluent, but its presence in sludges still presents a risk for WRF employees and may have implications for downstream handling of digester sludges (Wang et al., 2020). Employees for the Salt Lake City waste management have been notified of this fact and have been asked to take precautionary measures. Determining the abundance of SARS-CoV-2 in both sludge samples over time and in differing locations has proven valuable in monitoring changes in the epidemiological prevalence of COVID-19 (Lesimple et al., 2020). Overall, wastewater epidemiology addresses the variability in public health data introduced by factors such as asymptomatic carriers, hospital avoidance, privacy concerns, under-represented communities, and wide virus incubation times (Mao et al., 2020). Monitoring SARS-CoV-2 in wastewater has provided useful insight into the spread of COVID-19 on a state-wide scale (Weidhaas et al., 2021). However, wastewater tracking methods for SARS-CoV-2 might be improved by the examination of primary clarifier, return activated, or anaerobic digester sludges. Regardless of the matrix that is examined, wastewater surveillance for SARS-CoV-2 will inform and influence public policies that will ultimately save an unknown number of human lives.

Supplementary data to this article can be found online at https://doi.org/10.1016/j.scitotenv.2021.148905.

Declaration of competing interest

The authors declare that they have no known competing financial interests or personal relationships that could have appeared to influence the work reported in this paper.

Acknowledgement

We truly appreciate all the support provided by participating WRFs. Sampling at different locations of WRFs was critical and personnel from different WRFs unselfishly helped us with sampling. Most of the field sampling and student support was funded through The United States National Foundation's Rapid funding mechanism (Project # 2029515). However, the views presented in this manuscript are those of authors and not necessarily reflect on the funding agency. Partial funding through the University of Utah's I3 program provided partial support for student salary and molecular supplies.

References

Abboud, H., Abboud, F.Z., Kharbouch, H., Arkha, Y., El Abbadi, N., El Ouahabi, A., 2020. COVID-19 and SARS-CoV-2 infection: pathophysiology and clinical effects on the nervous system. World Neurosurgery 140, 49–53. https://doi.org/10.1016/j.wneu.2020.05.193.

Adhikari, S.P., Meng, S., Wu, Y.J., Mao, Y.P., Ye, R.X., Wang, Q.Z., et al., 2020. Epidemiology, causes, clinical manifestation and diagnosis, prevention and control of the coronavirus disease (COVID-19) during the early outbreak period: a scoping review. Infect. Dis. Poverty 9, 29. https://doi.org/10.1186/s40249-020-00646-x.

Ahmed, W., Harwood, V.J., Gyawali, P., Sidhu, J.P.S., Toze, S., 2015. Comparison of concentration methods for quantitative detection of sewage-associated viral markers in environmental waters. Appl. Environ. Microbiol. 81 (6), 2042–2049. https://doi.org/10.1128/AEM.03851-14.

Ahmed, W., Bertsch, P.M., Bivins, A., Bibby, K., Farkas, K., Gathercole, A., et al., 2020. Comparison of virus concentration methods for the RT-qPCR-based recovery of murine hepatitis virus, a surrogate for SARS-CoV-2 from untreated wastewater. Sci. Total Environ. 739, 139960. https://doi.org/10.1016/j.scitotenv.2020.139960.

Ahmed, W., Bibby, K., D'Aoust, P.M., Delatolla, R., ... Bivins, A., 2021. Differentiating between the possibility and probability of SARS-CoV-2 transmission associated with wastewater: empirical evidence is needed to substantiate risk. FEMS Microbes, 2 https://doi.org/10.1093/femsmc/xtab007.

Alygizakis, Nikiforos, 2016. Automatic detection of concentration trends of organic pollutants in wastewater using computational approaches and chemometric tools on data acquired by LC-HRMS. APHA (2005) Standard Methods for the Examination of Water and Waste Water, 21st edn American Public Health Association, Washington, DC.

Arslan, M., Xu, B., El-Din, M.G., 2020. Transmission of SARS-CoV-2 via fecal-oral and aerosols-borne routes: environmental dynamics and implications for wastewater management in underprivileged societies. Sci. Total Environ. 743, 140709. https://doi.org/10.1016/j.scitotenv.2020.140709.

Bogler, A., Packman, A., Furman, A., Gross, A., Kushmaro, A., Ronen, A., et al., 2020. Rethinking wastewater risks and monitoring in light of the COVID-19 pandemic. Nature Sustainability 3 (12), 981–990. https://doi.org/10.1038/s41893-020-00605-2.

Boogaerts, T., Jacobs, L., Roeck, N.D., Bogaert, S.V.d., Aertgeerts, B., Lahousse, L., Nuijs, A.L.N. van, Delputte, P., 2021. An alternative approach for bioanalytical assay optimization for wastewater-based epidemiology of SARS-CoV-2. Sci. Total Environ. 789, 148043. https://doi.org/10.1016/j.scitotenv.2021.148043.

Cahill, N., Morris, D., 2020. Recreational waters - a potential transmission route for SARS-CoV-2 to humans. Sci. Total Environ. 740, 140122. https://doi.org/10.1016/j.scitotenv.2020.140122.

Casanova, L., Rutala, W.A., Weber, D.J., Sobsey, M.D., 2009. Survival of surrogate coronaviruses in water. Water Res. 43, 1893–1898. https://doi.org/10.1016/j.watres.2009.02.002.

Chen, Y., Chen, L., Deng, Q., Zhang, G., Wu, K., Ni, L., et al., 2020. The presence of SARS-CoV-2 RNA in the feces of COVID-19 patients. J. Med. Virol. 92, 833–840. https://doi.org/10.1002/jmv.25825.

Cholankeril, G., Podboy, A., Aivaliotis, V.I., Pham, E.A., Spencer, S.P., Kim, D., Ahmed, A., 2020. Association of Digestive Symptoms and Hospitalization in patients with SARS-CoV-2 infection. Am. J. Gastroenterol. https://doi.org/10.14309/ajg.0000000000000712.

Cioabla, A.E., Ionel, I., Dumitrel, G.A., Popescu, F., 2012. Comparative study on factors affecting anaerobic digestion of agricultural vegetal residues. Biotechnology for Biofuels 5 (1), 1–9. https://doi.org/10.1186/1754-6834-5-39.

Corpuz, M.V.A., Buonerba, A., Vigliotta, G., Zarra, T., Ballesteros Jr, F., Campiglia, P., et al., 2020. Viruses in wastewater: occurrence, abundance, and detection methods. Sci. Total Environ. 745, 140910. https://doi.org/10.1016/j.scitotenv.2020.140910.

Dallas, T.A., Carlson, C.J., Poisot, T., 2019. Testing predictability of disease outbreaks with a simple model of pathogen biogeography. R. Soc. Open Sci. 6 (11). https://doi.org/10.1098/rsos.190883.

Doremalen, N.V., Bushmaker, T., Morris, D.H., Holbrook, M.G., Gamble, A., Williamson, B.N., et al., 2020. Aerosol and surface stability of SARS-CoV-2 as compared with SARS-CoV-1. N. Engl. J. Med. 382 (16), 1564–1567. https://doi.org/10.1056/NEJMc2004973.

Gu, J., Han, B., Wang, J., 2020. COVID-19: gastrointestinal manifestations and potential fecal-oral transmission. Gastroenterology 158 (6), 1518–1519. https://doi.org/10.1053/j.gastro.2020.02.054.

Gundy, P.M., Gerba, C.P., Pepper, I.L., 2009. Survival of coronaviruses in water and wastewater. Food Environ. Virol. 1, 10–14. https://doi.org/10.1007/s12560-008-9001-6.

Hata, A., Kitajima, M., Katayama, H., 2013. Occurrence and reduction of human viruses, F-specific RNA coliphage genogroups and microbial indicators at a full-scale wastewater treatment plant in Japan. J. Appl. Microbiol. 114, 545–554. https://doi.org/10.1111/jam.12051.

Hoseinzadeh, E., Javan, S., Farzadkia, M., Mohommadi, F., Hossini, H., Taghavi, M., 2020. An updated min-review on environmental route of the SARS-CoV-2 transmission. Ecotoxicol. Environ. Saf. 202. https://doi.org/10.1016/j.ecoenv.2020.111015.

Huang, Y., Zhou, B., Li, N., Li, Y., Han, R., Qi, J., et al., 2019. Spatial-temporal analysis of selected industrial aquatic heavy metal pollution in China. J. Clean. Prod. 238, 117944. https://doi.org/10.1016/j.jclepro.2019.117944.

Kitajima, M., Ahmed, W., Bibby, K., Carducci, A., Gerba, C.P., Hamilton, K.A., et al., 2020. SARS-CoV-2 in wastewater: state of the knowledge and research needs. Sci. Total Environ. 739, 139076. https://doi.org/10.1016/j.scitotenv.2020.139076.

Kocamemi, B.A., Kurt, H., Sait, A., Sarac, F., Saatci, A.M., Pakdemirli, B., 2020. SARS-CoV-2 Detection in Istanbul Wastewater Treatment Plant Sludges. MedRxiv.

Kumar, M., Taki, K., Gahlot, R., Sharma, A., Dhangar, K., 2020. A chronicle of SARS-CoV02: part-I-epidemiology, diagnosis, prognosis, transmission and treatment. Sci. Total Environ. 734, 139278. https://doi.org/10.1016/j.scitotenv.2020.139278.

La Rosa, G., Bonadonna, L., Lucentini, L., Kenmoe, S., Suffredini, E., 2020. Coronavirus in water environments: occurrence, persistence, and concentration methods - a scoping review. Water Res. 179, 115899. https://doi.org/10.1016/j.watres.2020.115899.

Lesimple, A., Jasim, S.Y., Johnson, D.J., Hilal, N., 2020. The role of wastewater treatment plants as tools for SARS-CoV-2 early detection and removal. Journal of Water Process Engineering 38, 101544. https://doi.org/10.1016/j.jwpe.2020.101544.

Lorenzo, M., Pico, Y., 2019. Wastewater-based epidemiology: current status and future prospects. Environ. Sci. Health 9, 77–84. https://doi.org/10.1016/j.coesh.2019.05.007.

Lu, X., Wang, L., Sakthivel, S.K., Whitaker, B., Murray, J., Kamili, S., et al., 2020. US CDC real-time reverse transcription PCR panel for detection of severe acute respiratory syndrome coronavirus 2. Emerg. Infect. Dis. 26 (8). https://doi.org/10.3201/eid2608.201246.

Mao, K., Zhang, K., Du, W., Ali, W., Feng, X., Zhang, H., 2020. The potential of wastewater-based epidemiology as surveillance and early warning of infectious disease outbreaks. Environmental Science and Health 17, 1–7. https://doi.org/10.1016/j.coesh.2020.04.006.

Medema, G., Heijnen, L., Elsinga, G., Italiaander, R., Brouwer, A., 2020. Presence of SARS-Coronavirus-2 RNA in sewage and correlation with reported COVID-19 prevalence in the early stage of the epidemic in the Netherlands. Environ. Sci. Technol. 7 (7), 511–516. https://doi.org/10.1021/acs.estlett.0c00357.

Metcalf and Eddy, 2014. Wastewater Engineering: Treatment and Resource Recovery. NY. McGraw-Hill Education, New York.

Peccia, J., et al., 2020a. Measurement of SARS-CoV-2 RNA in wastewater tracks community infection dynamics. Nat. Biotechnol. 38 (2020), 1164–1167.

Peccia, J., et al., 2020b. SARS-CoV-2 RNA Concentrations in Primary Municipal Sewage Sludge as a Leading Indicator of COVID-19 Outbreak Dynamics. *medRxiv*. https://doi.org/10.1101/2020.05.19.20105999.

Pecson, B.M., Darby, E., Haas, C.N., Amha, Y.M., Bartolo, M., Danielson, R., et al., 2021. Reproducibility and Sensitivity of 36 Methods to Quantify the SARS-CoV-2 Genetic Signal in Raw Wastewater: findings from an interlaboratory methods evaluation in the U.S. 7. Environ. Sci. Water Res. Technol., pp. 504–520.

Qui, X., 2012. Heat induced capsid disassembly and DNA release of bacteriophage λ. PLoS One 7 (7). https://doi.org/10.1371/journal.pone.0039793.

Randazzo, W., Truchado, P., Cuevas-Ferrando, E., Simon, P., Allende, A., Sanchez, G., 2020. SARS-CoV-2 RNA titers in wastewater anticipated COVID-19 occurrence in a low prevalence area. Water Res. 181. https://doi.org/10.1016/j.watres.2020.115942.

Sims, N., Kasprzyk-Hordern, B., 2020. Future perspectives of wastewater-based epidemiology: monitoring infectious disease spread and resistance to the community level. Environ. Int. 139, 105689. https://doi.org/10.1016/j.envint.2020.105689.

Sinclair, D.R., Grefenstette, J.J., Krauland, M.G., Galloway, D.D., Frankeny, R.J., Travis, C., et al., 2019. Forecasted size of measles outbreaks associated with vaccination exemptions for schoolchildren. JAMA Netw. Open 2 (8). https://doi.org/10.1001/jamanetworkopen.2019.9768 e199768–e199768.

Tozzoli, R., Di Bartolo, I., Gigliucci, F., Brambilla, G., Monini, M., Vignolo, E., et al., 2017. Pathogenic *Escherichia coli* and *enteric* viruses in biosolids and related top soil improvers in Italy. J. Appl. Microbiol. 122, 239–247. https://doi.org/10.1111/jam.13308.

Venugopal, A., Ganesan, H., Raja, S.S.S., Govindasamy, V., Arunachalam, M., Narayanasamy, A., et al., 2020. Novel wastewater surveillance strategy for early detection of coronavirus disease 2019 hotspots. Environ. Sci. Health 17, 8–13. https://doi.org/10.1016/j.coesh.2020.05.003.

Wang, J., Shen, J., Ye, D., Yan, X., Zhang, Y., Yang, W., et al., 2020. Disinfection technology of hospital wastes and wastewater: suggestions for disinfection strategy during coronavirus disease 2019 (COVID-19) pandemic in China. Environ. Pollut. 262, 114665. https://doi.org/10.1016/j.envpol.2020.114665.

Weidhaas, J., Aanderud, Z.T., Roper, D.K., VanDerslice, J., Gaddis, E.B., Ostermiller, J., et al., 2021. Correlation of SARS-CoV-2 RNA in wastewater with COVID-19 disease burden in sewersheds. Sci. Total Environ. 775. https://doi.org/10.1016/j.scitotenv.2021.145790.

Westhaus, S., Weber, F.-A., Schiwy, S., Linnemann, V., Brinkmann, M., Widera, M., ... Ciesek, S., 2021. Detection of SARS-CoV-2 in raw and treated wastewater inGermany–suitability for COVID-19 surveillance and potential transmission risks. Sci. Total Environ. 751, 141750. https://doi.org/10.1016/j.scitotenv.2020.141750.

Wigginton, K.R., Ye, Y., Ellenberg, R.M., 2015. Emerging investigators series: the source and fate of pandemic viruses in the urban water cycle. Environ. Sci. Water Res. Technol. 1, 735–746. https://doi.org/10.1039/C5EW00125K.

Wong, M.C., Huang, J., Lai, C., Ng, R., Chan, F.K., Chan, P.K., 2020. Detection of SARS-CoV-2 RNA in fecal specimens of patients with confirmed COVID-19: a meta-analysis. J. Inf. Secur. 81, e31–e38. https://doi.org/10.1016/j.jinf.2020.06.012.

Wrapp, D., Wang, N., Corbett, K.S., Goldsmith, J.A., Hsieh, C.L., Abiona, O., 2020. Cryo-EM structure of the 2019-nCoV spike in the prefusion conformation. Science 367 (6483), 1260–1263. https://doi.org/10.1126/science.abb2507.

WU, F.P., Man-qi, L.I.A.N.G., 2018. Analysis of industrial wastewater discharge and abatement potential in Jiangsu under total water consumption. China Population, Resources and Environment 8.

Wu, M.C., Sun, K.W., Zhang, Y., 2006. Influence of temperature fluctuation on thermophilic anaerobic digestion of municipal organic solid waste. Journal of Zhejiang University 7 (3), 180–185. https://doi.org/10.1631/jzus.2006.B0180.

Xagoraraki, I., O'Brien, E., 2020. Wastewater-based epidemiology for early detection of viral outbreaks. In: O'Bannon, D. (Ed.), Women in Water Quality. Women in Engineering and Science. Springer, Cham, pp. 75–97.

Yan, R., Zhang, Y., Li, Y., Xia, L., Guo, Y., Zhou, Q., 2020. Structural basis for the recognition of SARS-CoV-2 by full-length human ACE2. Science 367 (6485), 1444–1448. https://doi.org/10.1126/science.abb2762.

Ye, Y., Ellenberg, R.M., Graham, K.E., Wigginton, K.R., 2016. Survivability, partitioning, and recovery of enveloped viruses in untreated municipal wastewater. Environ. Sci. Technol. 50 (10), 5077–5085. https://doi.org/10.1021/acs.est.6b00876.

Zhang, J., Gao, Q., Zhang, Q., Wang, T., Yue, H., Wu, L., et al., 2017. Bacteriophage-prokaryote dynamics and interaction within anaerobic digestion processes across time and space. Microbiome 5 (1), 1–10. https://doi.org/10.1186/s40168-017-0272-8.